O(Mn) vibrational bands in double-layered manganites: First and second order Raman scattering

A. E. Pantoja,[1,3,*] H. J. Trodahl,[1] A. Fainstein,[2] R. G. Pregliasco,[2] R. G. Buckley,[3] G. Balakrishnan,[4] M. R. Lees,[4] and D. McK. Paul[4]

[1]*School of Chemical and Physical Sciences, Victoria University of Wellington, P.O. Box 600, Wellington, New Zealand*

[2]*Centro Atómico Bariloche, CNEA, 8400-San Carlos de Bariloche, Argentina*

[3]*Industrial Research Limited, P.O. Box 31310, Lower Hutt, New Zealand*

[4]*Department of Physics, University of Warwick, Coventry CV47AL, United Kingdom*

(Received 9 August 2000; published 13 March 2001)

The Raman spectra of a number of the colossal magnetoresistance manganites and related systems are shown to display strong broad vibrational bands in both first and second order. The modes derive from the entire phonon branch involving the vibration of the oxygen ions in the MnO_2 planes, ions which participate in Jahn-Teller displacements. The strength and temperature dependence of the second-order signal are shown to follow from conventional resonance scattering; they do not support the model that invokes Frank-Condon scattering.

DOI: 10.1103/PhysRevB.63.132406 PACS number(s): 75.30.Vn, 63.50.+x, 78.30.−j

I. INTRODUCTION

The colossal magnetoresistance (CMR) manganites have gained prominence recently for their application potential as well as their unusual magnetic and conducting behavior;[1,2] indeed they are a prototype for the complex behavior of the whole range of transition metal oxides.[3] Their magnetic and conducting properties are found to depend sensitively on the electronic correlations within the MnO_2 layers, as modulated by their crystallographic structure and the Mn valance. Raman spectroscopy is particularly well suited to studies of the structure and electronic contributions to bonding in these weakly conducting materials and in this paper we report detailed Raman measurements on several crystals of the CMR and related manganites.

The most frequently studied CMR manganites are the pseudocubic versions, doped perovskites $(La,A)MnO_3$, with $A=$ Sr, Ca. On first glance one would expect at most a very weak Raman signal from these manganites, for without their relatively weak noncubic distortions there would be no Raman active vibrational modes at all. That expectation is nearly true, for the strong lines in the spectra in doped materials are very broad; the only narrow phonon peaks are indeed weak.[4–13]

In contrast, stoichiometric $LaMnO_3$ (LMO) shows Raman lines, which though still weak, are all narrow at and below ambient temperature.[13–16] Those lines in the stoichiometric material have been confidently assigned on the basis of experimental symmetry determinations and lattice dynamics. In the doped versions of the materials, on the contrary, there is less agreement among authors as to either the detailed spectra or their interpretation. The situation is not aided by the fact that much of the experimental work has been performed on polycrystalline ceramics or thin films, and in both cases there is the potential that the spectra are confused by rogue phases.

In line with general trends in the field most Raman studies on the manganites have concentrated on doped pseudocubic materials $La_{1-x}Sr_xMnO_3$ and $La_{1-x}Ca_xMnO_3$ (LCMO). From the point of view of Raman spectroscopy the double-layer manganites of the Ruddlesen-Popper series $R_{2-2x}Sr_{1+2x}Mn_2O_7$, (R-327, $R=$ rare earth)[1] appear to be a more attractive proposition than the pseudocubic form. Not only do they have Raman active modes,[17–19] even in the absence of distortions from their ideal tetragonal structure, but in addition they have been prepared with a range of phase diagrams, displaying ferromagnetic, antiferromagnetic, charge-ordering and metal-insulator transitions.[20–24]

In this paper we report spectra of bilayered R-327 for $R=(La,Pr,Nd,Dy)$ and $x\leqslant 0.5$, and relate them to published reports on the pseudocubic materials of similar doping. Although the spectra from all these systems differ in the details of their weak, narrow, zone-center phonon lines, there is a remarkable similarity among the materials in the behavior of the two broad features across the $400-800\ cm^{-1}$ region. We suggest below that these features are from the entire O(Mn) vibrational band, rendered Raman active by orientational disorder in the Jahn-Teller (JT) displacements of the O(Mn) ions.

II. EXPERIMENTAL DETAILS

Single crystals of the layered manganites were grown by the floating zone method using an infrared image furnace as described elsewhere.[25] Raman experiments were conducted on cleaved surfaces using Jobin-Yvon T64000 and U1000 monochromators with the 514.5, 488, 647.1, and 676.4 nm lines from Ar^+ and Kr^+ lasers. The samples were mounted in vacuum in a closed cycle helium refrigerator.

In Table I we present the magnetic and conducting properties[25–30] of the seven single crystals for which we have spectra. It is notable that the magnetic and conducting states in these crystals span the entire range found in the manganites except that none of them correspond to doping states for which all Mn ions are in the triple-valance state in which a fully ordered cooperative JT state is expected.

III. RESULTS AND DISCUSSION

A. First-order scattering

In Fig. 1 we display low-temperature spectra of a selection of the samples, at $T\sim 30$ K in $z(x'x')\bar{z}$ polarization

TABLE I. Studied R-327 systems with their magnetic and electronic phases, from Refs. 25–30. All samples are paramagnetic insulators at 295 K. The temperatures denote ferromagnetic (T_C), antiferromagnetic (T_N), spin-glass freezing (T_F), and insulator-to-metallic (T_{IM}) transitions. The axes (abc) denote which orientation the transition is seen in and * denotes a weak transition.

R	x	T_C	T_N	T_F	T_{IM}
La	0.4	120 K (ab)	–	–	120 K (ab)
Nd	0.25	280 K (abc)	190 K* (ab)	50 K (c)	125 K* (ab) 90 K* (c)
Nd	0.4	–	–	43 K (c)	–
Pr	0.4	–	–	45 K (c)	–
Pr	0.5	–	130 K (ab)	25 K (abc)	–
Dy	0.4	–	–	–	–
Dy	0.5	–	–	30 K (c)	–

(using the Porto notation) with both incident and scattered light polarized along the Mn-O bonds. Note that these double-layered crystal data are all on basal-plane surfaces; c-axis spectra are substantially different and will be published separately. Equivalent data on the pseudocubic crystals are presented elsewhere.[31] These and all subsequent data curves have been divided by the Bose-Einstein correction factor $[n(\omega,T)+1]=[1-\exp(-\hbar\omega/k_BT)]^{-1}$ to account for the sample's temperature, though in our data this correction has only a small effect above 400 cm^{-1}.

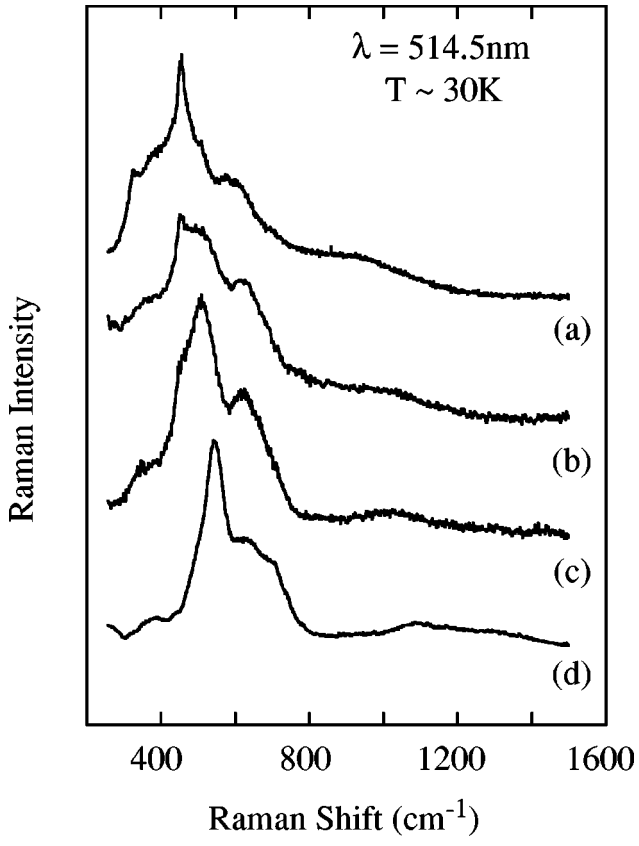

FIG. 1. Low-temperature Raman spectra of R-327. (a) R=Pr, x=0.5, (b) R=La, x=0.4, (c) R=Dy, x=0.4, and (d) R=Nd, x=0.4; taken in the $z(xx)\bar{z}$ polarization, normalized and offset for clarity. Data in all other basal-plane polarization configurations also show the broad features in the 400−800 cm^{-1} spectral region.

There are differences in detail between the spectra from the various samples and polarizations, but what is most striking is the similarity as regards the presence of broad bands between 400 and 800 cm^{-1}. The similarity persists through the series despite the widely differing structural, magnetic and conducting states displayed at these temperatures. A similar pattern is found in previously published spectra from the doped manganites.[4–13,17–19]

There is controversy concerning the assignment in earlier reports of the broad features in the 400−800 cm^{-1} range. Their commonality among the nonlayered pseudocubic materials has been noted,[6] and based in part on their frequent appearance it has been suggested they are zone-center modes rendered Raman active by disorder in the Jahn-Teller distortions within the MnO_2 planes.[5] However it has not been explicitly recognized that their appearance does not depend on the long-range crystallographic order; to the contrary their absence in stoichiometric LMO in its uniform collective JT ground state, suggests that they rely on the randomly oriented JT distortions expected in any of the materials with mixed Mn valance. On the other hand, even stoichiometric LMO spectra show broad lines across 400−800 cm^{-1} at temperatures approaching the 800 K collective JT transition on the Mn^{3+} sites.[8,16]

Clearly the presence of the disorder introduced either by elevated temperatures or by doping is required to observe the features. It is important to note that in either case the reorientation is local, and can be expected to provide coupling to the entire vibrational band related to the JT displacements, rather than to simply the zone-center modes. Thus we assign the broad modes between 400−800 cm^{-1} to scattering from a full phonon branch involving the vibrations of oxygen ions in the MnO_2 planes.

B. Second-order scattering

Recently[32,33] it has been suggested that a 2 eV excitation in stoichiometric LMO involves a local atomic rearrangement that rotates the JT displacements about one Mn site in the cooperative JT ground state. Based on that picture a strong second-order Raman signal is predicted. The argument is that the reorientation of the JT O-ion displacements forms a self-trapped exciton, which is described by a superposition of coupled electronmultiphonon states. Strong Raman activity to second and higher order is then predicted to occur via Frank-Condon scattering.

The first-order results described in the previous paragraphs are not in disagreement with the model proposed by Allen and Perebeinos. We turn now to higher frequencies, where all of the crystals show second-order scattering seen clearly in Fig. 1. The predictions concerning the strength of that second-order scattering are quite different for Frank-Condon as opposed to conventional Raman scattering, so that these spectra provide a test for the Allen and Perebeinos model.

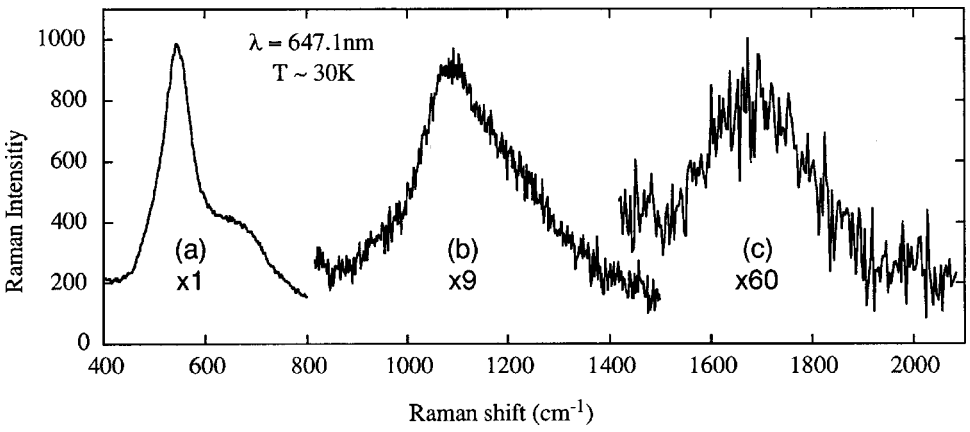

FIG. 2. Multiple-order scattering in $Nd_{1.2}Sr_{1.8}Mn_2O_7$ ($x=0.4$). (a) First-order signal unmodified, (b) and (c) second- and third-order scattering with a sloped linear offset subtracted, magnified as shown for clarity.

In common with LCMO,[31] $Nd_{1.2}Sr_{1.8}Mn_2O_7$ has a strong second-order signal, which was measurable over the whole temperature range; most of the others had a signal that rose clearly above the background only below 200 K. That higher-order signal is a simple doubling and tripling of the original frequency of the entire broad feature between 400 -800 cm^{-1}, as shown in Fig. 2. Also, it is only the broad non-zone-center O(Mn) modes that are repeated in higher order. For instance, we find no evidence of the sharp polarization-dependent mode at 450 cm^{-1} in $PrSr_2Mn_2O_7$ and $La_{1.2}Sr_{1.8}Mn_2O_7$ (previously assigned to an in-phase O_{xy} bending mode[17]) being represented at higher order. Since it is only the O(Mn) modes that appear in second order, we seek evidence as to whether Frank-Condon scattering is responsible for that second-order signal.

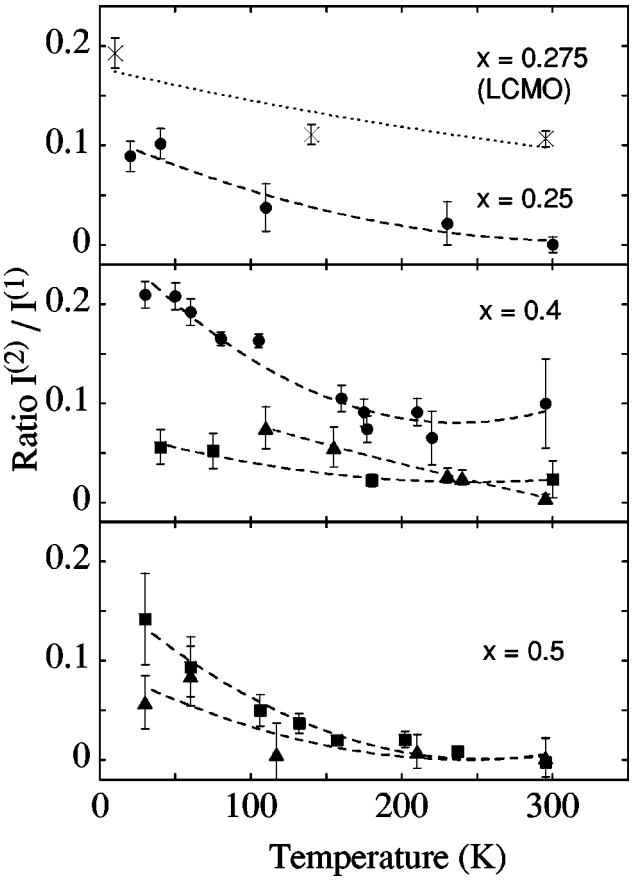

FIG. 3. Temperature dependence of the second- to first-order spectral integrated intensity ratio with $\lambda=514$ nm from crystals with differing Mn^{4+} fractions x, as labelled. *Solid symbols*: R-327 for Nd (circles), Dy (triangles), and Pr (squares). *Crosses*: an estimate of the integrated intensity ratio for LCMO with $x=0.275$ from Ref. 31. The lines are guides to the eye.

As a quantitative charaterization of the first- and second-order Raman signals, we have compared the ratio of their corresponding spectral integrated signal strengths. For first order this is $I^{(1)}=\int d\omega\, S^{(1)}(\omega)$, integrated above a sloping linear background and across the broad first-order bands in the region $400-800$ cm^{-1}. Similarly, we have calculated $I^{(2)}=\int d\omega\, S^{(2)}(\omega)$ across matching doubled-frequency limits where we find the second-order signal. In Fig. 3 we plot the ratio $I^{(2)}/I^{(1)}$ between these two integrated signal strengths, where it can be seen that the ratio clearly falls with increasing temperature. Also, the weakening of $I^{(2)}$ does not appear to be correlated in any way with specific phase transitions, nor does it appear to be strongly dependent on the low-temperature phase. Furthermore, it does not show the temperature-independent behavior expected from the Frank-Condon mechanism.[32–34] To the contrary, the increasing second-order signal at low temperatures can be understood on the basis of conventional resonant Raman scattering. Within this picture it arises from an increase at low temperatures of the lifetime of the resonant excitation, the trapped exciton in the Allen and Perebeinos picture.

The amplitude of the resonance is a stronger function of that lifetime in $I^{(2)}$ than in $I^{(1)}$ due to an extra energy term in the denominator of the Raman susceptibility,[34] and exactly on resonance the Raman intensity ratio ($I^{(2)}/I^{(1)}$) is then proportional to the square of the lifetime of the excited state. It is important to recognize that all of our crystals are expected to have disordered JT states, with the excitation energy varying among the various Mn^{3+} sites. In the resulting inhomogeneously broadened resonance the lifetime dependence will persist over the entire resonant profile. Thus the temperature dependence of Fig. 3 can be understood as reflecting only the temperature dependence of the square of the exciton lifetime.

We have conducted a search for resonance effects in $Nd_{1.2}Sr_{1.8}Mn_2O_7$ across the 488–647 nm (1.92–2.54 eV) range, which has revealed no significant changes to the spec-

trum or its temperature dependence. In particular, contrary to an earlier report,[11] we find no new features appearing between 514.5 and 488 nm, so that the both first- and second-order signals of the $400-800\ \mathrm{cm}^{-1}$ band can easily be identified in all low-temperature spectra from our crystals. At $T \sim 30$ K the ratio $I^{(2)}/I^{(1)}$ increases by about 30% in going from 1.92 to 2.54 eV, approximately as predicted by Perebeinos *et al.*[33] However, the magnitude of the ratio is an order of magnitude smaller than expectations following from the Frank-Condon process.[33] This observation lends further evidence for conventional, rather than Frank-Condon exciton-mediated resonant Raman scattering.

IV. CONCLUSION

To summarize, we have reported first- and second-order Raman signals in a wide range of manganite crystals. The spectra show a similarity that suggests that the intense broad lines on which we have focused cannot depend on the detailed magnetic, metallic, or charge-ordered state. We assign the features to vibrations in the common element, Mn-O octahedra. The broad nature of the features is consistent with scattering from a full vibrational branch, suggesting in turn that the photon-phonon coupling mechanism involves a local interaction. The presence of a second-order signal is in agreement with a mechanism associated with a local exciton as suggested by Allen and Perebeinos,[32,33] but its magnitude and temperature dependence establishes that it involves conventional resonant Raman scattering rather than the Frank-Condon effect.

ACKNOWLEDGMENTS

A.E.P. would like to thank Centro Atómico Bariloche, Argentina, for hospitality during his visit. We are grateful for support from the New Zealand Marsden Fund.

*Corresponding address: Materials Physics, Industrial Research Limited, P.O. Box 31310, Lower Hutt, New Zealand. Email address: o.pantoja@irl.cri.nz

[1] A.P. Ramirez, J. Phys.: Condens. Matter **9**, 8171 (1997).
[2] M. Imada *et al.*, Rev. Mod. Phys. **70**, 1039 (1998).
[3] Y. Tokura and N. Nagaosa, Science **288**, 462 (2000).
[4] E. Liarokapis *et al.*, Phys. Rev. B **60**, 12 758 (1999).
[5] M.V. Abreshev *et al.*, Phys. Rev. B **59**, 4146 (1999).
[6] M. V. Abrashev *et al.*, Phys. Status Solidi B **215**, 631 (1999).
[7] S. Yoon *et al.*, Phys. Rev. B **58**, 2795 (1998).
[8] V.B. Podobedov *et al.*, Phys. Rev. B **58**, 43 (1998).
[9] V.B. Podobedov *et al.*, Appl. Phys. Lett. **73**, 3217 (1999).
[10] J.C. Irwin *et al.*, Phys. Rev. B **59**, 9362 (1999).
[11] V. Dediu *et al.*, Phys. Rev. Lett. **84**, 4489 (2000).
[12] P. Björnsson *et al.*, Phys. Rev. B **61**, 1193 (2000).
[13] E. Granado *et al.*, Phys. Rev. B **58**, 11 435 (1998).
[14] M.N. Iliev *et al.*, Phys. Rev. B **57**, 2872 (1998).
[15] E. Granado *et al.*, Phys. Rev. B **60**, 11 879 (1999).
[16] E. Granado *et al.*, Phys. Rev. B **62**, 11 304 (2000).
[17] D.B. Romero *et al.*, Phys. Rev. B **58**, 14 737 (1998).
[18] D.N. Argyriou *et al.*, Phys. Rev. B **61**, 15 269 (2000).
[19] K. Yamamoto *et al.*, Phys. Rev. B **61**, 14 706 (2000).
[20] R.I. Bewley *et al.*, Phys. Rev. B **60**, 12 286 (1999).
[21] Y. Moritomo, Aust. J. Phys. **52**, 255 (1999).
[22] N.H. Hur *et al.*, Phys. Rev. B **57**, 10 740 (1998).
[23] T. Kimura *et al.*, Phys. Rev. Lett. **81**, 5920 (1998).
[24] P.D. Battle *et al.*, J. Mater. Chem. **7**, 977 (1997).
[25] G. Balakrishnan *et al.*, J. Phys.: Condens. Matter **9**, 471 (1997).
[26] J.F. Mitchell *et al.*, Phys. Rev. B **55**, 63 (1997).
[27] B. García-Landa *et al.*, Phys. Rev. B **60**, 5440 (1999).
[28] B. García-Landa *et al.*, Phys. Rev. Lett. **84**, 995 (2000).
[29] G. Balakrishnan (private communication).
[30] B. García-Landa (private communication).
[31] A. E. Pantoja *et al.* (unpublished).
[32] P.B. Allen and V. Perebeinos, Phys. Rev. Lett. **83**, 4828 (1999).
[33] V. Perebeinos and P.B. Allen, cond-mat/0007301 (unpublished).
[34] M. Cardona, in *Light Scattering in Solids II*, edited by M. Cardona and G. Güntherdot, Topics in Applied Physics, Vol. 50 (Springer-Verlag, Berlin, 1982).